Korean J. Chem. Eng., 39(1), 63-68 (2022)
DOI: 10.1007/s11814-021-0987-x
pISSN: 0256-1115
eISSN: 1975-7220

RAPID COMMUNICATION

Plasma etching of SiO_2 contact hole using perfluoropropyl vinyl ether and perfluoroisopropyl vinyl ether

Sanghyun You, Jun-Hyun Kim, and Chang-Koo Kim†

Department of Chemical Engineering and Department of Energy Systems Research,
Ajou University, Worldcup-ro 206, Yeongtong-gu, Suwon 16499, Korea
(*Received 29 September 2021 • Revised 14 October 2021 • Accepted 18 October 2021*)

Abstract−Perfluoropropyl vinyl ether (PPVE) and perfluoroisopropyl vinyl ether (PIPVE) are used for plasma etching of SiO_2 contact holes. When etching is performed on blanket SiO_2 samples, the etch rates in the PPVE/Ar plasma are higher than those in the PIPVE/Ar plasma at all bias voltages. In contrast, when hole-pattern (100 nm in diameter) SiO_2 samples are etched, the etch rates of the SiO_2 hole in the PIPVE/Ar plasma are higher than those of the SiO_2 hole in the PPVE/Ar plasma. This can be attributed to excess production of CF_3^+ ions in PIPVE than in PPVE, and higher contribution of physical sputtering to plasma etching in PIPVE than in PPVE. The angular dependence of the SiO_2 etch rates examined using a Faraday cage reveals that the effect of physical sputtering on the SiO_2 etching is greater in the PIPVE/Ar plasma than in the PPVE/Ar plasma.

Keywords: Plasma Etching, Contact Hole, PPVE, PIPVE, Angular Dependence

INTRODUCTION

Plasma etching of SiO_2 has attracted attention owing to the increasing demand for a high-aspect-ratio SiO_2 contact hole during the fabrication of semiconductor devices. Perfluoro compounds (PFCs), such as carbon tetrafluoride (CF_4) and octafluorocyclobutane (c-C_4F_8), are mainly used as discharge materials for the plasma etching of SiO_2 [1-4]. PFCs have a high global warming potential (GWP), long atmospheric lifetime, and strong infrared absorption. According to the Fifth Assessment Report of the Intergovernmental Panel on Climate Change (IPCC), the 100-year time horizon GWPs of CF_4 and c-C_4F_8 is 6630 and 9540, respectively. Because PFCs cause environmental problems, worldwide efforts have been made to reduce PFC emissions. One method is to replace PFCs with low-GWP alternatives, such as hydrofluorocarbons [5], iodofluorocarbons [6,7], hydrofluoroethers [8,9], and perfluoroalkyl vinyl ethers [10-12].

Perfluoroalkyl vinyl ethers have drawn attention because of their extremely low GWPs. The presence of unsaturated sites and hydrogen atoms in perfluoroalkyl vinyl ethers increases the reactivity of the molecules into hydroxyl radicals [13]. Although several perfluoroalkyl vinyl ethers have been examined as alternatives to PFCs for the plasma etching of SiO_2, there are few reports on SiO_2-contact-hole etching using perfluoroalkyl vinyl ethers, and their etch characteristics are still unclear.

In this study, perfluoropropyl vinyl ether (PPVE) and perfluoroisopropyl vinyl ether (PIPVE) are examined for the plasma etching of a SiO_2 contact hole, and their etch characteristics are compared at various bias voltages. PPVE and PIPVE belong to the group of perfluoroalkyl vinyl ethers and their GWP is approximately 3, which is significantly lower than that of PFCs. As they are isomers, their molecular formulae are identical and structural formulae are different. In each plasma, blanket SiO_2 samples and hole-pattern (100 nm diameter) SiO_2 samples are etched to investigate the etch characteristics of the SiO_2 contact hole. The angular dependence of the SiO_2 etch rates in the plasmas using PPVE and PIPVE is compared to investigate the etch mechanisms.

EXPERIMENTAL

SiO_2 etching was conducted in an inductively coupled plasma (ICP) chamber, which is described in previous studies [9,14]. Separate 13.56-MHz radio-frequency (rf) power generators were used to independently control the density and energy of ions produced in the plasma.

The ICP chamber was equipped with a Faraday cage to measure the etch rates of SiO_2 at various ion-incident angles. The use of a Faraday cage facilitates the control of the ion-incident angle (θ), which is defined as the angle between the direction of the ion incidence and the surface normal to the substrate. The principles and applications of the Faraday cage are described in previous studies [15,16].

PPVE and PIPVE were used as discharge materials, and their typical properties are listed in Table 1. They have identical molecular formulae ($C_5F_{10}O$), but different structures. As the boiling point of PPVE and PIPVE is 35 °C, they exist in liquid phase at room temperature. Therefore, they were vaporized in canisters, and the vaporized PPVE and PIPVE flowed with Ar as the carrier gas. Then, the mixtures PPVE/Ar and PIPVE/Ar were introduced into the ICP chamber.

The PPVE/Ar and PIPVE/Ar plasmas, respectively, were used for the SiO_2 etching. The bias voltage was varied from −400 to −1,000 V.

†To whom correspondence should be addressed.
E-mail: changkoo@ajou.ac.kr

Table 1. Typical properties of PPVE and PIPVE

Name	Perfluoropropyl vinyl ether (PPVE)	Perfluoroisopropyl vinyl ether (PIPVE)
Structural formula	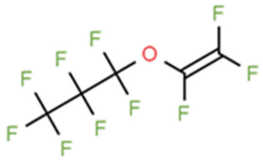	
Molecular formula	$C_5F_{10}O$	
Boiling point (°C)	35.0	
Global warming potential	3	

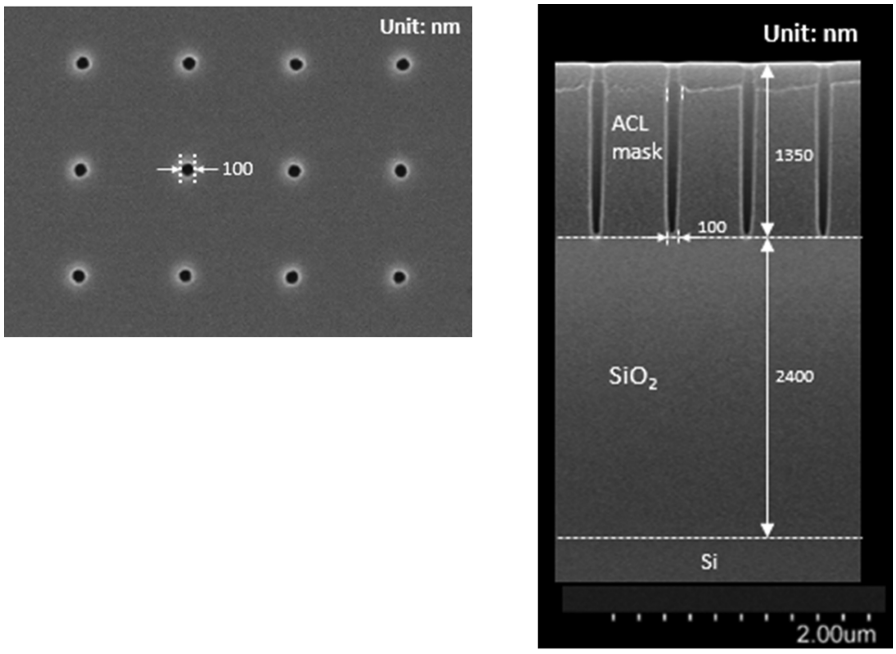

(a) (b)

Fig. 1. (a) Top and (b) cross-sectional SEM images of patterned sample. The sample had a pattern of 100 nm-diameter holes.

Other process conditions were fixed as follows: 250 W source power, 10 mTorr chamber pressure, 10 sccm PPVE flow rate, 10 sccm PIPVE flow rate, and 20 sccm Ar flow rate.

SiO_2 etching was performed using either a blanket or a patterned sample. The blanket sample was a 500-nm-thick SiO_2 film on a silicon wafer. The patterned sample was a silicon substrate, which consisted of a SiO_2 film with a hole pattern (100 nm diameter). The top and cross-sectional views of the patterned samples are shown in Fig. 1. A pattern of 100-nm-diameter holes was delineated using an amorphous carbon layer (ACL) as a mask. The thicknesses of the SiO_2 film and ACL mask were 2,400 and 1,350 nm, respectively.

The etch rates of the blanket samples were obtained by measuring the thickness changes of the blanket substrate film before and after etching using a thickness meter (K-MAC, ST2000-DLXn). The etch profiles of the patterned samples were obtained using field-emission scanning electron microscopy (FE-SEM, Hitachi S-4800).

RESULTS AND DISCUSSION

Fig. 2 shows the change in the etch rates of the blanket SiO_2 samples with the bias voltage in the PPVE/Ar and PIPVE/Ar plasmas. The etch rates monotonically increased with the increase in bias voltage in both plasmas. This was expected because the energy of ions bombarding the surface of the substrate increased with the increase in bias voltage. The etch rates of the blanket SiO_2 samples in the PPVE/Ar plasma were higher than those of the blanket SiO_2 samples in the PIPVE/Ar plasma at all bias voltages used in this study.

Fig. 3 shows the SEM images of the patterned SiO_2 samples etched in the PPVE/Ar and PIPVE/Ar plasmas at various bias voltages. In all cases, the etching time was 12 min. The etch profiles of the hole patterns revealed the occurrence of highly anisotropic etching using the PPVE/Ar and PIPVE/Ar plasmas. The etch depths of the SiO_2 hole in the PIPVE/Ar plasma were deeper (or the etch

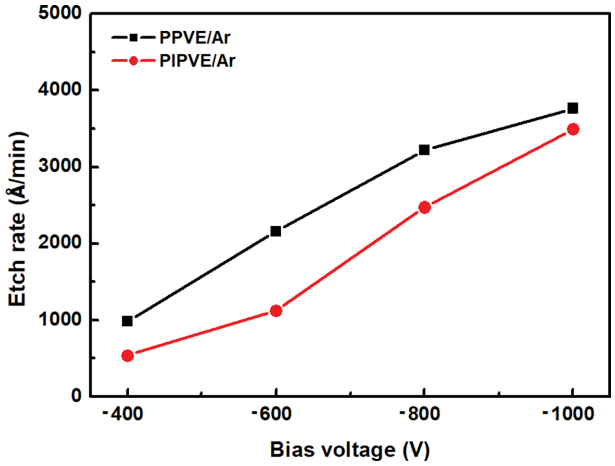

Fig. 2. Change in etch rates of blanket SiO_2 samples with bias voltage in PPVE/Ar and PIPVE/Ar plasmas.

rates of the SiO_2 hole were higher) than those of the SiO_2 hole in the PPVE/Ar plasma at all bias voltages used in this study. This result contradicts etch rates of the blanket SiO_2 samples. In the case of the blanket SiO_2 samples, the PIPVE/Ar plasma led to a lower etch rate than the PPVE/Ar plasma.

A possible reason for the relative predominance of the etch rates between the PPVE/Ar and PIPVE/Ar plasmas is the shape of the sample (either blanket or patterned) owing to the etch mechanism (either physical sputtering or ion-enhanced chemical etching) in each plasma. A plasma is a partially ionized gas that consists of electrons, ions, and neutrals. During plasma etching, complex reactions, such as sputtering by ions, chemical etching by neutral radicals, and ion-assisted reactions, occur simultaneously. Depending on the process conditions and types of discharge materials, one of the etch mechanisms (either physical sputtering or ion-enhanced chemical etching) is dominant over others.

As PPVE and PIPVE are isomers of each other, the only difference between them is the molecular structure. Considering their molecular structures, excessive CF_3^+ ions are produced in the PIPVE than in the PPVE plasma. Karahashi et al. measured the etch yield of SiO_2 for F^+, CF^+, CF_2^+, and CF_3^+ ions with energies ranging from 250 to 2,000 eV [17]. They reported that the etch yield of CF_x^+ (x=1, 2, 3) ions increased with an increasing number of F atoms in the incident ions. Thus, CF_3^+ ions exhibited the highest etch yield. Because excessive CF_3^+ ions were generated in the PIPVE plasma than in the PPVE plasma, the etch yield was expected to be higher in the PIPVE plasma than in the PPVE plasma. This implies that the contribution of physical sputtering was higher in the PIPVE plasma than in the PPVE plasma.

As mentioned, a plasma consists of electrons, ions, and neutrals. During plasma etching, a substrate is negatively charged with respect to the bulk plasma. Thus, positive ions arrive at the substrate in the direction normal to the surface of the substrate. In contrast, neutrals do not travel in the preferred direction and arrive at the substrate in all directions. When a patterned sample is exposed to a plasma, the selected area, which is not covered by a mask, is etched. Considering the fluxes of the ions and neutrals to the surfaces of the blanket and patterned samples, respectively, the flux of ions to the surface of the unit etchable area is the same for both types of samples. In contrast, the flux of neutrals to the surface of the unit etchable area is lower for the patterned samples than it is for the blanket samples. This is illustrated in Fig. 4. Therefore, the etched SiO_2 films experience a higher ion-to-neutral ratio for the

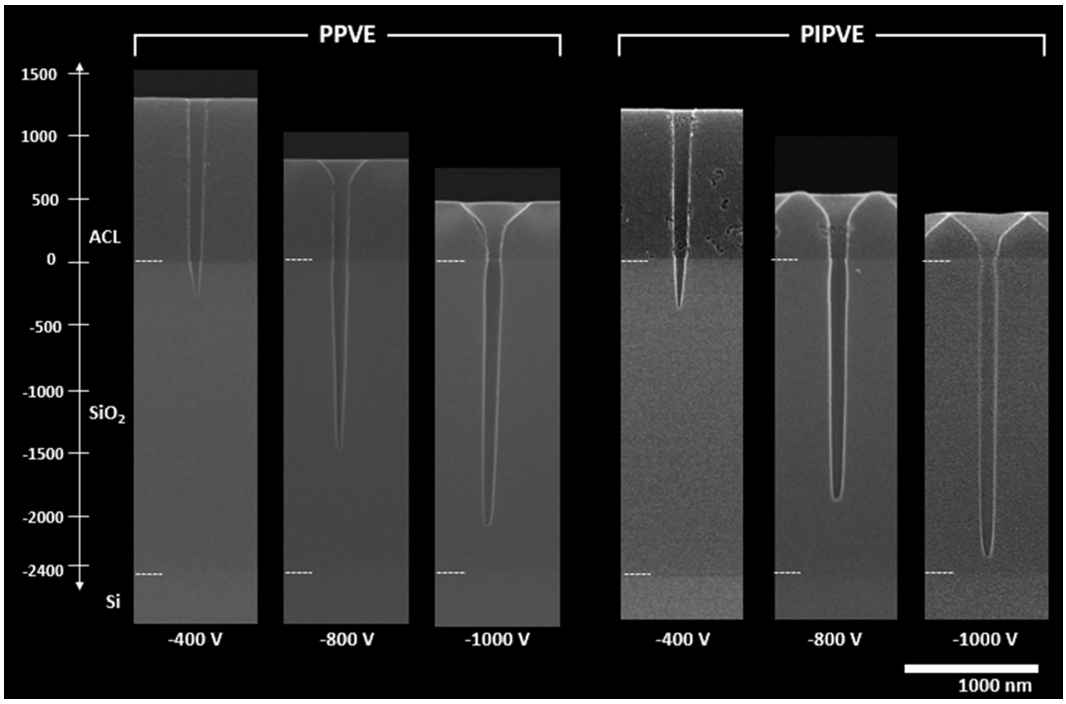

Fig. 3. SEM images of patterned SiO_2 samples etched in PPVE/Ar and PIPVE/Ar plasmas, respectively, at various bias voltages.

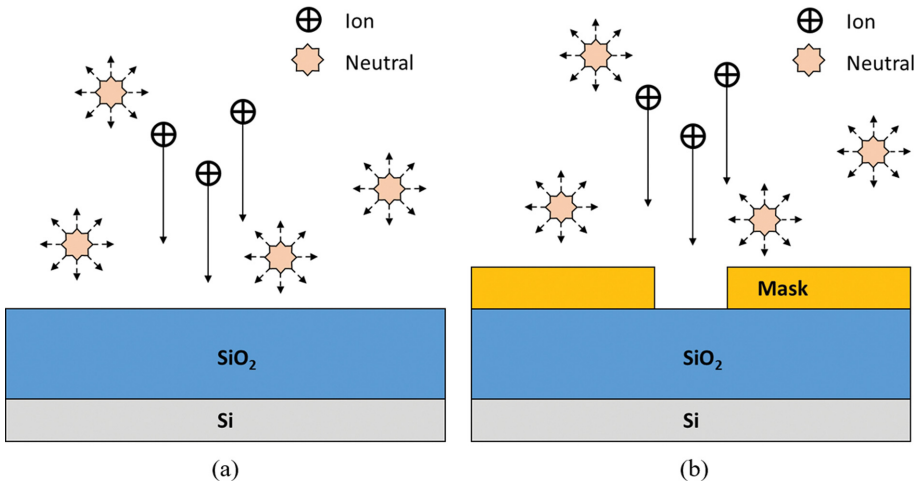

Fig. 4. Schematic of fluxes of ions and neutrals to the surface of (a) blanket and (b) patterned samples during plasma etching.

patterned samples than the blanket ones. Because the contribution of physical sputtering to the etch mechanism is prominent when the ion-to-neutral ratio is high, the etch yield (even etch rate) of the patterned sample is higher in the PIPVE than in the PPVE plasmas. This explanation for the higher etch rates of the patterned sample in the PIPVE plasma than in the PPVE plasma is valid only if the contribution by physical sputtering is higher in the PIPVE plasma than in the PPVE plasma. To determine the dominant etch mechanism (physical sputtering or ion-enhanced chemical etching) among the PIPVE and PPVE plasmas, the etch rates of SiO_2 at various ion-incident angles were obtained using the Faraday cage.

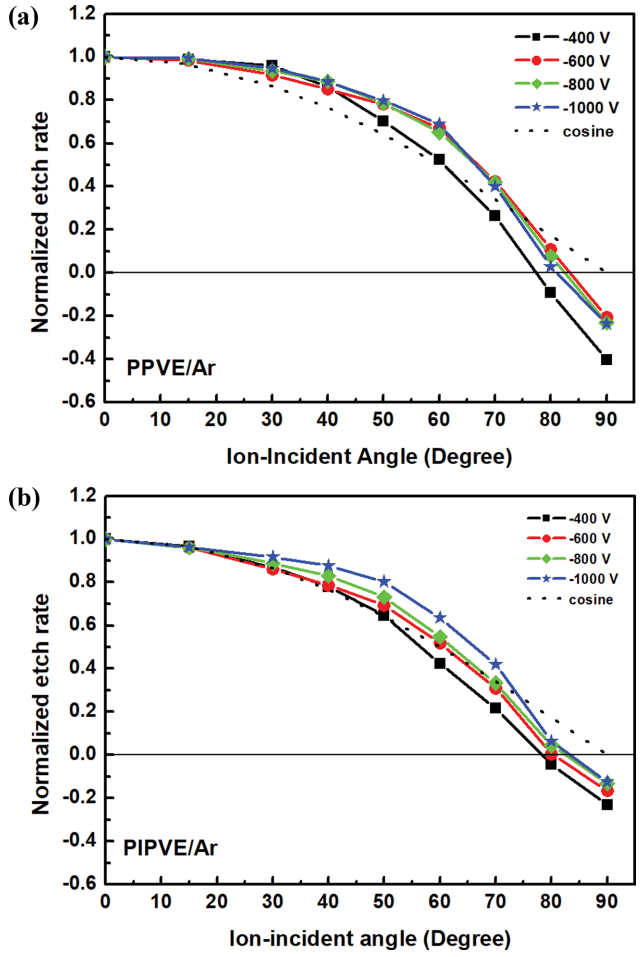

Fig. 5. Change in normalized etch rates of SiO_2 with ion-incident angle in (a) PPVE/Ar plasma and (b) PIPVE/Ar plasmas at various bias voltages.

Fig. 5 shows the change in the normalized etch rates (NERs) of SiO_2 with the ion-incident angle in the PPVE/Ar and PIPVE/Ar plasmas at various bias voltages. The NER is defined as the etch rate at a specific angle normalized with respect to the etch rate on the horizontal surface, that is, etch rate (θ)/etch rate (0°). In both plasmas, the NERs had a maximum value of unity at the ion-incident angle of 0°, implying that the etch rate of SiO_2 was maximum when the direction of the ion incidence was normal to the surface of the substrate. In addition, the NERs of SiO_2 monotonically decreased with the increase in ion-incident angle at all bias voltages in both plasmas. The continuous decrease in NERs with the increase in ion-incident angle resulted in film deposition (negative value of NER) at the ion-incident angle of 90°. In the PPVE/Ar plasma, the NERs were virtually distributed on a single curve for the bias voltages higher than −600 V. In contrast, the NERs in the PIPVE/Ar plasma increased with the increase in bias voltage. The NER curves of the two plasmas imply that the effect of the bias voltage (corresponding to ion energy) on SiO_2 etching was stronger in the PIPVE/Ar plasma than in the PPVE/Ar plasma.

The angular dependence of the etch rate is affected by the ion flux variation because the change in the flux of ions with their incidence angles follows the cosine curve. To examine ion-surface interactions at various ion-incident angles, it is necessary to exclude ion flux variations with ion-incident angles. Because the etch yield is the etch rate per ion flux on the substrate, the etch yield is used to compare the etch mechanisms in the PPVE/Ar and PIPVE/Ar plasmas rather than the etch rate.

Fig. 6 shows the angular dependence of the normalized etch yield (NEY) of SiO_2 in the PPVE/Ar and PIPVE/Ar plasmas at

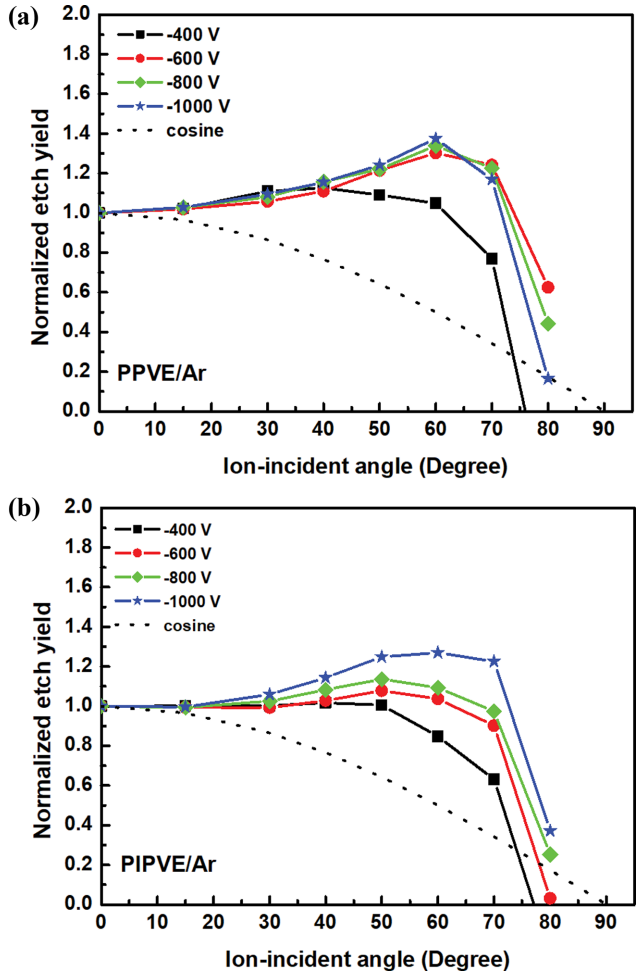

Fig. 6. Angular dependence of normalized etch yields of SiO_2 in (a) PPVE/Ar and (b) PIPVE/Ar plasmas at various bias voltages.

various bias voltages. The NEY is defined as the etch yield at a specific angle normalized with respect to the etch yield on the horizontal surface, that is, etch yield (θ)/etch yield (0°). Therefore, the etch yield is equal to NER/cosθ. In both plasmas, the NEY increases with the increase in ion-incident angle and reaches the maxima at angles between 40° and 60°. Further, the NEY decreases with the increase in ion-incident angle. During plasma etching, physical sputtering is considered to be the dominant etch mechanism when the etch yield is maximum at angles between 40° and 70° [18]. Therefore, we can conclude that the SiO_2 etching in the PPVE/Ar and PIPVE/Ar plasmas is mainly contributed by the physical etching rather than the ion-enhanced chemical etching.

However, the dependence of the NEY on the bias voltage suggests that the effect of physical sputtering on the SiO_2 etching in the PPVE/Ar and PIPVE/Ar plasmas is different. In the PPVE/Ar plasma, the NEY curves were almost unaffected up to the ion incident angle of 70° at the bias voltages from −600 to −1,000 V. This implies that the effect of the ion energy is negligible at the bias voltages higher than −600 V. However, the NEYs in the PIPVE/Ar plasma continuously increased with the increase in bias voltage, indicating that ion energy affected this plasma. Because ion energy is an important parameter in physical sputtering, the dependence of the NEYs on the bias voltage (or ion energy) indicates that the contribution of physical sputtering to the SiO_2 etching is higher in the PIPVE/Ar plasma than in the PPVE/Ar plasma. This resulted in a higher etch yield (or even etch rate) of the patterned sample in the PIPVE/Ar plasma than in the PPVE/Ar plasma, as shown in Fig. 3.

CONCLUSIONS

SiO_2 etching was performed on PPVE/Ar and PIPVE/Ar plasmas at various voltages (−400 to −1,000 V) using blanket and patterned samples. When performed on the blanket SiO_2 samples, the etch rates in the PPVE/Ar plasma were higher than those in the PIPVE/Ar plasma at all bias voltages. In contrast, when the hole pattern (100 nm in diameter) SiO_2 samples were etched, the etch rates of the SiO_2 hole in the PIPVE/Ar plasma were higher than those of the SiO_2 hole in the PPVE/Ar plasma.

The relative predominance of the etch rates of the patterned samples between the PPVE/Ar and PIPVE/Ar plasmas was attributed to the etch mechanism in each plasma. The angular dependence of the SiO_2 etch rates examined using the Faraday cage in the PPVE/Ar and PIPVE/Ar plasmas at various bias voltages showed that the NEYs reached their maxima at ion-incident angles between 40° and 60° in both plasmas. This implies that the SiO_2 etching in the PPVE/Ar and PIPVE/Ar plasmas was mainly contributed by physical etching rather than ion-enhanced chemical etching. Although physical etching majorly contributed to the SiO_2 etching in both plasmas, the contribution of physical sputtering to the SiO_2 etching was different in PPVE/Ar and PIPVE/Ar plasmas. The NEYs were almost unaffected up to an ion-incident angle of 70° at bias voltage from −600 to −1,000 V in the PPVE/Ar plasma, while they continuously increased with the bias voltage in the PIPVE/Ar plasma. Because ion energy is a critical parameter in physical sputtering, the dependence of the NEYs on the bias voltage (corresponding to the ion energy) indicated that the effect of physical sputtering on the SiO_2 etching is greater in the PIPVE/Ar plasma than in the PPVE/Ar plasma. Then, owing to the higher ion-to-neural flux of the patterned sample, the prominent contribution of physical sputtering to the etching mechanism in the PIPVE/Ar plasma resulted in a higher etch yield (even etch rate) of the patterned sample in the PIPVE/Ar plasma than in the PPVE/Ar plasma.

ACKNOWLEDGEMENTS

This work was supported by the National Research Foundation of Korea (NRF) grant funded by the Korean government (MEST) (grant No. 2021R1A2B5B01001836) and the GRRC program of Gyeonggi province (GRRC AJOU 2016B03, Photonics-Medical Convergence Technology Research Center).

REFERENCES

1. J.-H. Kim, S.-W. Cho, C. J. Park, H. Chae and C.-K. Kim, *Thin Solid Films*, **637**, 43 (2017).
2. B.-O. Cho, S.-W. Hwang, G.-R. Lee and S. H. Moon, *J. Vac. Sci.*

Technol. A, **18**, 2791 (2000).
3. J.-K. Lee, G.-R. Lee, J.-H. Min and S. H. Moon, *J. Vac. Sci. Technol. A*, **25**, 1395 (2007).
4. J.-H. Kim and C.-K. Kim, *Korean J. Chem. Eng.*, **37**, 374 (2020).
5. S. Karecki, L. Pruette, R. Reif, T. Sparks, L. Beu and V. Vartanian, *J. Electrochem. Soc.*, **145**, 4305 (1998).
6. F. Fracassi and R. d'Agostino, *J. Vac. Sci. Technol. B*, **16**, 1867 (1998).
7. S. Samukawa, T. Mukai and K.-I. Tsuda, *J. Vac. Sci. Technol. A*, **17**, 2551 (1999).
8. Y. Chinzei, Y. Feurprier, M. Ozawa, T. Kikuchi, K. Horioka, T. Ichiki and Y. Horiike, *J. Vac. Sci. Technol. A*, **18**, 158 (2000).
9. J.-H. Kim, J.-S. Park and C.-K. Kim, *Thin Solid Films*, **669**, 262 (2019).
10. Y. Morikawa, W. Chen, T. Hayashi and Y. Uchida, *Jpn. J. Appl. Phys.*, **42**, 1429 (2003).
11. M. Nagai, T. Hayashi, M. Hori and H. Okamoto, *Jpn. J. Appl. Phys.*, **45**, 7100 (2006).
12. J.-H. Kim, J.-S. Park and C.-K. Kim, *ECS J. Solid State Sci. Technol.*, **7**, Q218 (2018).
13. B. Allgood, *Adv. Mater.*, **10**, 1239 (1998).
14. J.-H. Kim, J.-S. Park and C.-K. Kim, *Appl. Surf. Sci.*, **669**, 262 (2019).
15. J.-H. Kim, S.-W. Cho and C.-K. Kim, *Chem. Eng. Technol.*, **40**, 2251 (2017).
16. S.-W. Cho, C.-K. Kim, J.-K. Lee, S. H. Moon and H. Chae, *J. Vac. Sci. Techmol. A*, **30**, 051301 (2012).
17. K. Karahashi, K.-I. Yanai, K. Ishikawa, H. Tsuboi, K. Kurihara and M. Nakamura, *J. Vac. Sci. Techmol. A*, **22**, 1166 (2004).
18. D. P. Hamblen and A. Cha-Lin, *J. Electrochem. Soc.*, **135**, 1816 (1988).